

# Microstructure and Wear Resistance of Al<sub>2</sub>O<sub>3</sub> Coatings on Functional Structure

Chao-Ping JIANG<sup>1,2,a</sup>, Xiang-Ze KONG<sup>1,b</sup>, Ya-Zhe XING<sup>1,c</sup>,  
Jian-Min HAO<sup>1,d</sup> and Xu-Ding SONG<sup>2,e</sup>

<sup>1</sup>School of materials science and engineering, Chang'an University, Xi'an, 710064, China;

<sup>2</sup>Key laboratory of road construction technology and equipment MOE

<sup>a</sup>jcp100415@126.com<sup>1</sup>, <sup>b</sup>18792591623@163.com, <sup>c</sup>xingyz@chd.edu.cn, <sup>d</sup>h-jianmin@126.com, <sup>e</sup>songxd@chd.edu.cn

**Abstract.** To enhance the wear properties of function structure, Al<sub>2</sub>O<sub>3</sub>-13%TiO<sub>2</sub> (AT13) coatings were plasma sprayed on 45 steel functional structure using micro and nano powders. The microstructures and phase compositions of the coatings were investigated by scanning electron microscopy and X-ray diffraction, respectively. Results show that the nano powder coating consists of fully-melted region and partially-melted region. The fully-melted regions show a lamellar structure, while the partially-melted regions retain the powders structure. The phases of coatings are  $\alpha$ -Al<sub>2</sub>O<sub>3</sub> and TiO<sub>2</sub>. The wear test was carried out on a ML-10 friction and wear tester under dry sliding condition. It is found that the wear resistance of the micro powder coating is higher than that of nano powder coating. This is mainly ascribe to the breakage of the nano powder coating resulted from low agglomerated binding force.

## 1. Introduction

In transportation machinery and equipment, much functional structure must work in harsh environment, especially in insufficient lubricated conditions. Many ceramic coatings can protect these structure parts effectively<sup>[1,2]</sup>. Al<sub>2</sub>O<sub>3</sub> coatings are widely studied for their useful performance such as high hardness, high melting point and excellent erosion resistance and wear resistance<sup>[3]</sup>. However, for practical applications, the low brittleness of Al<sub>2</sub>O<sub>3</sub> ceramics limits its applications. To solve this problem, low melt point materials are often added into Al<sub>2</sub>O<sub>3</sub> coatings to form composite coatings. It is believed that TiO<sub>2</sub> can improve the mechanical properties of the composite coating<sup>[4]</sup>. It is believed that the composite ceramic with 13wt% TiO<sub>2</sub> can maintain the balance between toughness and plasticity properties<sup>[5,6]</sup>. Vargas<sup>[7]</sup> studied the Al<sub>2</sub>O<sub>3</sub>-TiO<sub>2</sub> ceramic coatings fabricated by flame and air plasma spray (FS and APS). Their results show that coatings with denser structure and high mechanical properties can be fabricated by APS. APS is supposed to be an ideal method to deposit AT13 coating.

In this study, two types of composite coatings were prepared by APS using micro and nano AT13 feedstock. The relationship between the microstructure and wear properties of the two coatings were investigated.

---

\* Corresponding author: jcp100415@126.com

## 2. Experimental

45 steel was chosen as the substrate material, which was cut into rectangular samples with a size of 30 mm×15 mm×3 mm. Prior to spraying, the substrate was degreased in acetone and grit blasted using virgin brown alumina particles with an average diameter of 1-3 mm.

AT13 coatings were deposited on steel surfaces by a GP-80 APS system using micro and nano powders. Argon and hydrogen was used as primary gas and auxiliary gas respectively. The spraying parameters are listed in Table 1. In the process of plasma spraying, the substrate was heated to 300°C by plasma arc in order to increase the bonding strength.

The micro powders feedstock (with a size of 15-55 μm) was fused and crushed, as shown in Fig.1a. The nano powders with a spherical morphology was agglomerated and sintered, as shown in Fig. 1b. The average size of nano powders is about 50 μm.

**TABLE 1 ATMOSPHERIC PLASMA SPRAYING PARAMETERS**

Parameter	Condition
Spraying current/A	600
Spraying volage/V	70
Argon gas pressure/MPa	0.7
Hydrogen gas pressure/MPa	0.68
Argon gas flow/L · min <sup>-1</sup>	45
Hydrogen gas flow/L · min <sup>-1</sup>	8
Feed rate/g · min <sup>-1</sup>	10
Spraying distance/mm	100
Coating thickness/μm	200-300

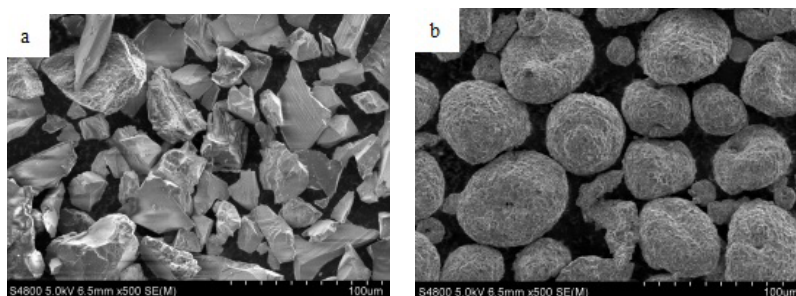


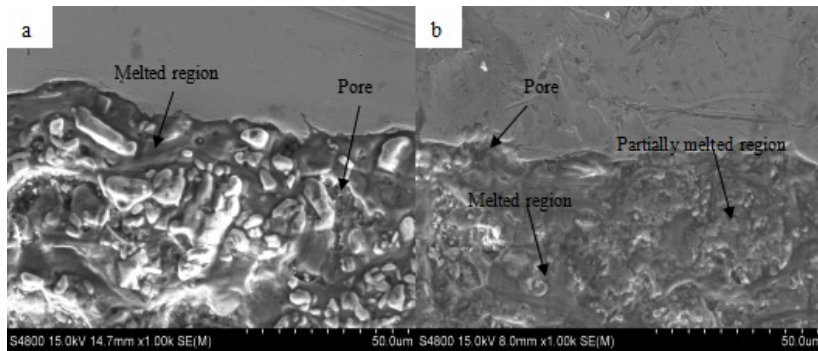
**Fig. 1 SEM images of the (a) micro powders (b) nano powders**

The cross-sectional structure of the samples was characterized by scanning electron microscopy (SEM, S-4800). X-ray diffraction (XRD, X'Pert Pro) analysis was performed on an X-ray diffractometer with CuKα radiation. Wear tests were conducted on a ML-10 Pin on disc friction testing machine under dry sliding condition. The wear resistance of the ceramic composite coatings was characterized by mass loss and worn surfaces SEM analysis.

### 3. Results and Discussion

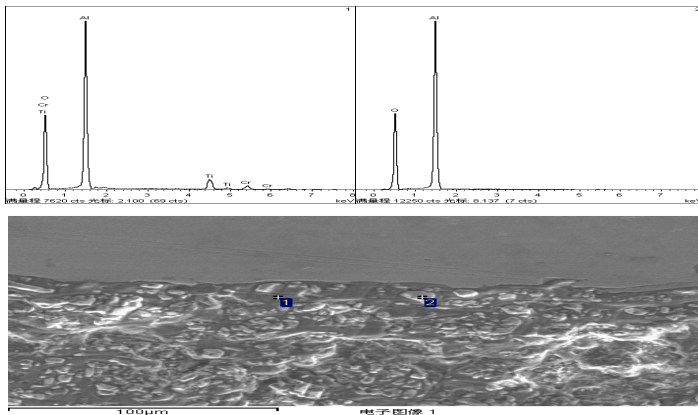
#### 3.1 Microstructure of the Coatings

Fig. 2 presents the cross-section SEM images of the plasma-sprayed AT13 coatings. The substrates and coatings are located at the top and the bottom of the graphs, respectively. Because the materials of coating and substrate are different, the structure of the AT13 coatings are composed of lamellar structure, partially-melted powders and pores. Large particles were embedded in the melted region, as shown in Fig. 2a. The size of particles is larger than 5  $\mu\text{m}$ . The nano powder coating consists of both fully-melted and partially-melted regions in the same spray parameters, as shown in Fig. 2b, which is identical with published literatures<sup>[8-10]</sup>. The nano powders particle agglomerates from many nano particles, and there are plenty of interfaces. Many pores exist in agglomerated particle, which can block the heat transfer from the outer into the inner region. Thus, the exterior of the particle could be well melted together, while the inner of the particle keeps the starting structure.



**Fig.2 Cross-sectional SEM morphologies of AT13 coatings made from (a) micro powders and (b) nano powders**

The EDS analysis of the micro powder coating is shown in Fig. 3. According to the EDS results, the chemical elements at point 1 are mainly Al, Ti, O and Cr. Cr comes from the polishing agent  $\text{Cr}_2\text{O}_3$ . It is identified that the coatings are composed of  $\text{Al}_2\text{O}_3$  and  $\text{TiO}_2$ . The white particles at point 2 consist of Al and O, which means the coating is consisted of  $\text{Al}_2\text{O}_3$ .



**Fig.3 EDS spectra of the micro powder coating at different points**

### 3.2 Phase Composition of the Micro and Nano Powder Coatings

The phase structure of the plasma-sprayed AT13 coatings is presented in Fig. 4. It is evident that both the micro and nano powder coatings are composed of  $\text{TiO}_2$ ,  $\gamma\text{-Al}_2\text{O}_3$  and  $\alpha\text{-Al}_2\text{O}_3$ . The only difference between the two coatings is the relative diffraction intensity, which can be explained by the nucleation kinetics. Compared with nano powder coating (Fig. 4b), the metastable  $\gamma\text{-Al}_2\text{O}_3$  phase in micro powder coating (Fig. 4a) is easier to form, because the cooling rate of the micro powders is different from nano powder coating. The metastable  $\gamma\text{-Al}_2\text{O}_3$  phase in micro powder coating is larger than that of the nano powder coating. With a sufficient cooling rate, the metastable  $\gamma\text{-Al}_2\text{O}_3$  phase is easy to form at room temperature<sup>[11]</sup>. For the agglomerate powder with many gaps, the nano powders would have a low thermal conductivity.

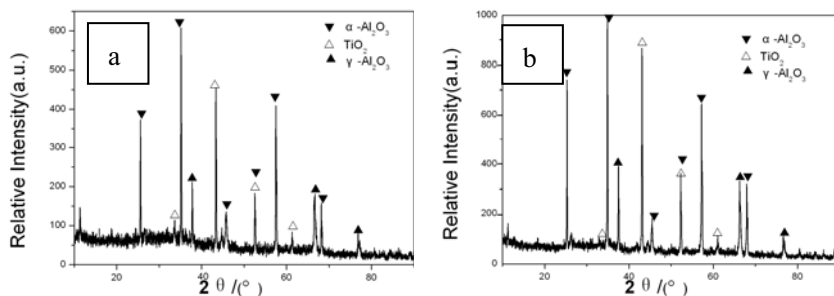


Fig. 4 XRD patterns of the micro powder (a) and nano powder (b) coatings

### 3.3 Wear Performance

Fig. 5 illustrates the wear behaviors of the micro and nano powder coatings under dry condition. The mass loss of the nano powder coating is much higher than that of the micro powder coating, especially with high loads. This phenomenon can be explained as follows. Though the existence of melted regions in the nano powder coatings is helpful to improve ductility and fracture toughness<sup>[12]</sup>, the melted regions only exist in exterior of the particles and the intersplat bond force is not strong enough to resist the wear stress in dry wear condition. If the exterior melted regions of the particles are broken, the whole splats maybe stripped during friction, as shown in Fig. 6b.

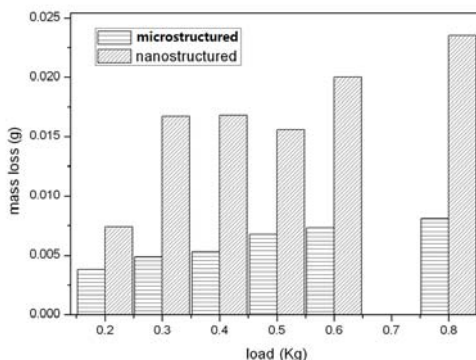


Fig. 5 The mass loss of two coatings with different loads

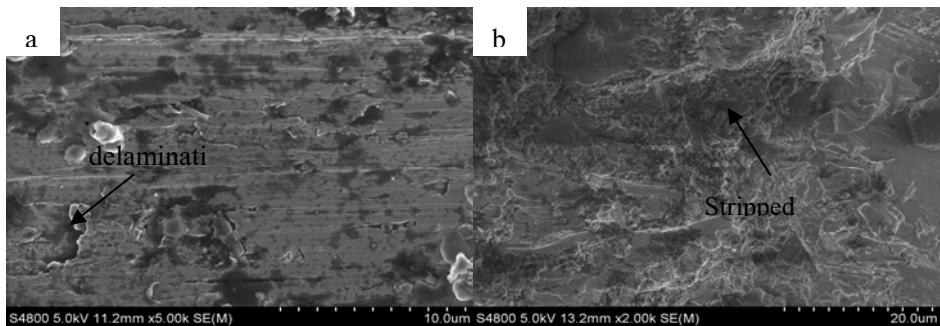
The micro powder coating shows good wear resistance because hard  $\text{Al}_2\text{O}_3$  particles

resist wear stress and the melted region (contain much of  $TiO_2$ ) envelop the hard particles. On the one hand, the melted regions fix the hard  $Al_2O_3$  particles and prevent it from pulling out from the coatings during the wear process. On the other hand, the  $Al_2O_3$  particles have very high hardness and well wear resistance. There are only few delaminations appeared in worn surface of the micro powder coating, as shown in Fig. 6a. The pore defect is an unavoidable feature, so the delaminations can be easy formed on the pores, and the spraying splats have lower bond strength.

## 4. Conclusions

The as-sprayed micro powder coating shows lamellar stacking characteristic and has some pores. However, the as-sprayed nano powder coating consists of both fully-melted regions and partially-melted regions. It is convinced that the nano powder coating has poor wear resistance under dry condition because the nano powders particles are easy to be striped from the coating surface. The micro powder coating with the characteristics of the particulate-reinforced composite materials shows good wear resistance. So the micro powder  $Al_2O_3$  coatings can be used to protect function structure in dry friction.

**Fig.6 SEM images of the worn surface of (a) micro powder and (b) nano powder coatings**



## 5. Acknowledgements

This work was financially supported by the Special Found for Basic Scientific Research of Central Colleges, Chang'an University (310831161005, 310831161018).

## References

1. Deng S. J. Thermal sprayed high performance ceramic coatings, *J. materials protection*. 1999,32(1):31-34.
2. Xu C. S., Wang H. S., Zhou X.J. et al. The corrosion resistance status quo and prospect of thermal sprayed coatings on metal surface, *J. materials protection*. 2011, 44(10):59-62.
3. Vargas F, Ageorges H, Fournier P. Mechanical and tribological performance of  $Al_2O_3$ - $TiO_2$  coatings elaborated by flame and plasma spraying, *J. Surface & Coatings Technology*. 2010, 205(5-6):1132-6.
4. Yilmaz R., Kurt A., Demir A., Tatli, Effects of  $TiO_2$  on the mechanical properties of the  $Al_2O_3$ - $TiO_2$  plasma sprayed coating, *J. Journal of the European Ceramic Society*. 2007, 27: 1319-1323.

5. Lu L., Ma Z., Wang F. C., Liu Y. B. Friction and wear behaviors of Al<sub>2</sub>O<sub>3</sub>-13 wt%TiO<sub>2</sub> coatings, *J. Rare Met.* 2013. 32(1):87-92.
6. Goberman D, Sohn Y. H., Shaw L., Jordon E., Gell M. Microstructure development of Al<sub>2</sub>O<sub>3</sub>-13 wt%TiO<sub>2</sub> sprayed coatings derived from nano crystalline powders, *J. J Acta Mater.* 2002. 50(5):1141-1152.
7. F. Vargas, H. Ageorges, P. Fournier, P. Fauchais, M.E. López. Mechanical and tribological performance of Al<sub>2</sub>O<sub>3</sub>-TiO<sub>2</sub> coatings elaborated by flame and plasma spraying, *J. Surface & Coatings Technology.* 2010, 205 : 1132-1136.
8. Lima R.S., Kucuk A., Berndt C.C., and Gell M., Bimodal distribution of mechanical properties on plasma sprayed nanostructured partially stabilized zirconia, *J. Material Science and Engineering. A*, 2002, 327 (2): 224.
9. Zhang J., He J., Dong Y., et al. Microstructure and properties of Al<sub>2</sub>O<sub>3</sub>-13wt.%TiO<sub>2</sub> coatings sprayed using nanostructured powders, *J. Rare Metals*, 2007, 26 (4): 391-397.
10. Wang D. S., Tian Z. J., Shen L. D., et al. Preparation and characterization of nanostructured Al<sub>2</sub>O<sub>3</sub>-13wt.% TiO<sub>2</sub> ceramic coatings by plasma spraying, *J. Rare Metals*. 2009, 28(5): 465-470.
11. Qian J. G., Zhang J. X., Xu M., et al. Characterization and Corrosion Resistance of Laser Cladding Al<sub>2</sub>O<sub>3</sub>-13%TiO<sub>2</sub> Coating on AZ91D Magnesium Alloy, *J. Rare Metal Materials and Engineering.* 2011, 40(S4): 221-225.
12. Song E.P., Ahn J., Lee S. and Kim N.J., Effects of critical plasma spray parameter and spray distance on wear resistance of Al<sub>2</sub>O<sub>3</sub>-8wt.%TiO<sub>2</sub> coatings plasma-sprayed with nanopowders, *J. Surface & Coatings Technology*, 2008, 202 (15): 3625.16-17.